Magneto-optical effects of excitons in BiI_3 crystals under pulsed high magnetic fields. III. Excitons confined around a stacking disorder formed by a bending stress

K. Watanabe,* S. Takeyama,† and N. Miura
Institute for Solid State Physics, University of Tokyo, Roppongi, Minato-ku, Tokyo 106, Japan

T. Komatsu, T. Higashimura,‡ and T. Iida
Department of Physics, Faculty of Science, Osaka City University, Sumiyoshi-ku, Osaka 558, Japan
(Received 3 May 1993; revised manuscript received 11 October 1993)

We have observed a series of lines in the absorption and luminescence spectra of BiI_3 crystals which are strained by a bending stress. The magnetic-field effects on these lines were investigated in pulsed high magnetic fields up to 47 T. The magneto-optical spectra were well explained by the cationic exciton model. The origin of the lines was concluded to be an exciton state confined around a stacking disorder, which was formed by deformation. We discuss the quantum size effect of the excitons in the specific region of the stacking disorder.

I. INTRODUCTION

The optical absorption edge of BiI_3 crystals is governed by an allowed indirect exciton transition[1] and a direct exciton transition which occurs at slightly higher energy.[2] Several sharp exciton absorption lines Q, R, S, and T are observed below the absorption edge. In two previous papers, which are denoted as Papers I (Ref. 3) and II (Ref. 4), magneto-optical effects of these excitons have been presented. The magnetic-field effects on the direct and the indirect excitons are well explained by the cationic exciton model in Paper I. In Paper II, the magneto-optical effects on the Q, R, S, and T lines were investigated in detail. We found that the origins of the Q, R, S, and T lines are exciton states localized around a stacking fault,[5] and that the localized states originate from the cationic exciton states.[6] Throughout these investigations, we have demonstrated that magneto-optical measurements in high magnetic fields are a very powerful means to study the internal structure of small-radius excitons.

In the absorption spectra of BiI_3 crystals, another sharp line, called W, was found under special conditions.[7] The W line appears in the transparent region of the absorption spectra. The W line is induced by deforming the crystal with a bending stress. Since the W line appears under different conditions from those accounting for the appearance of the P, Q, R, S, and T lines, the origin of the W line is considered to be different from those of the P, Q, R, S, and T lines. We have reported preliminary results of the magnetoabsorption (MA) spectra of the W line.[8] Lisitsa and Motsnyi reported the observation of luminescence peaks near the energy position of the W line.[9]

In this paper, we study a series of peaks including the W line in the absorption and luminescence spectra in pulsed high magnetic fields. Magneto-optical behavior of the series of lines is interpreted by the cationic exciton model. The energy levels of the lines have been calculated by a tight-binding model. In recent years, exciton systems confined in microcrystals or thin layers have attracted much attention from the viewpoint of optical nonlinear materials.[10] We propose that the present lines originate from exciton states confined in the vicinity of stacking disorders, and that these excitons exhibit quantum size effects.

II. EXPERIMENTAL PROCEDURE

Single crystals of BiI_3 were grown by a sublimation method.[1] The W line is not usually observed in as-grown samples. After deforming a crystal with a bending stress, the W line appears in the absorption and luminescence spectra. Thin flakes of single crystals whose absorption spectra exhibit the W line were selected for optical measurements.

Luminescence spectra were excited by a He-Ne laser or an Ar-ion laser. Magneto-absorption spectra were obtained by using a system combining a single-grating spectrometer, an optical fiber system, and an optical multichannel analyzer (OMA). Details of the MA measurement have been presented in Paper I.

The magnetoluminescence (ML) measurement is as follows. Radiation of a line from an Ar-ion laser was used for the excitation. Light pulses were formed by a mechanical chopper from the cw laser radiation. The pulse width was chosen to be slightly longer than the gate time of the OMA. The gate of the OMA was opened at the maximum of a pulsed magnetic field. The exciting light was led to the sample holder through a fiber bundle. The luminescence from the samples was introduced to the spectrometer also through a fiber bundle. A colored glass filter was set behind the entrance slit in the spectrometer to cut out the exciting light.

The measurements were carried out with several different configurations of the magnetic field $\mathbf{B}$, the crystal

c axis **z**, the polarization **E**, and the wave vector of the incident light **k**;[11] the [**B**⊥**z**, **k**||**z**] and the [**B**||**z**, **k**||**z**] configurations with nonpolarized incident light, and the [**B**⊥**z**, **B**||**E**, **k**||**z**] and the [**B**⊥**z**, **B**⊥**E**, **k**||**z**] configurations with linearly polarized incident light. Since the samples used in the present work are thin along the **z** axis (the direction of the layer stacking), optical spectra were measured only in the **k**||**z** configuration.

III. EXPERIMENTAL RESULTS

A. Absorption and luminescence spectra

The W absorption line appears on the lower-energy side of the indirect exciton absorption edge of BiI_3 crystals. We rename the W line as the W^{I} line in the present paper for the sake of convenience in the following discussion. W^{I} was not observed before deforming the crystal, as shown in spectrum a of the inset in Fig. 1. The crystal was carefully deformed step by step, and the spectrum was measured after each step. Spectra b–d were obtained during such a process. The absorption intensity of W^{I} became larger and larger at each step, while its energy position did not change. These spectra were measured under stress-free conditions. Therefore, the stress itself is not the cause of the W^{I} line. When the crystal was more strongly deformed, the spectrum in Fig. 1(a) was obtained. The absorption intensity of W^{I} became very large, and two new absorption lines, W^{II} and W^{III}, appeared on the lower-energy side of the W^{I} line. The absorption intensities of the W^{J} (J=I,II,III) lines decreased with increasing J. The energy positions of W^{I}, W^{II}, and W^{III} were 1.931, 1.878, and 1.850 eV, respectively, at 4.2 K.

The luminescence spectra were measured in the same energy region of the W^{J} absorption lines. Figure 1(b) shows the luminescence spectrum obtained for a strongly deformed sample. The sample was excited by the 632.8-nm line of the He-Ne laser. Luminescence lines were observed at the energy positions of the W^{I}, W^{II}, and W^{III} lines. These luminescence lines can be labeled as W^{I}, W^{II}, and W^{III}, respectively. At energies below those of the W^{I}, W^{II}, and W^{III} luminescence lines, other luminescence lines were observed. These luminescence lines were labeled as $W^{I'}$, $W^{II'}$, and $W^{III'}$. No absorption lines were clearly observed at the energy positions of the $W^{I'}$, $W^{II'}$, and $W^{III'}$ lines.

B. Magnetoabsorption spectra

The MA spectra of the W^{I} and W^{II} lines were measured in pulsed high magnetic fields. The MA spectra in the [**B**⊥**z**, **k**||**z**] configuration depend on the polarization of the incident light. Figure 2 shows the MA spectra both in the [**B**⊥**z**, **B**||**E**, **k**||**z**] and in the [**B**⊥**z**, **B**⊥**E**, **k**||**z**] configurations obtained by using linearly polarized incident light. The W^{I} line exhibited splitting in the magnetic field. The split lines at the lower- and higher-energy sides were labeled as W_1^{I} and W_2^{I} lines, respectively. W_2^{I} was observed for **B**||**E**, and not for **B**⊥**E**. W_1^{I} was observed for **B**⊥**E**, and not for **B**||**E**. Furthermore, two new weak lines were found to be induced by

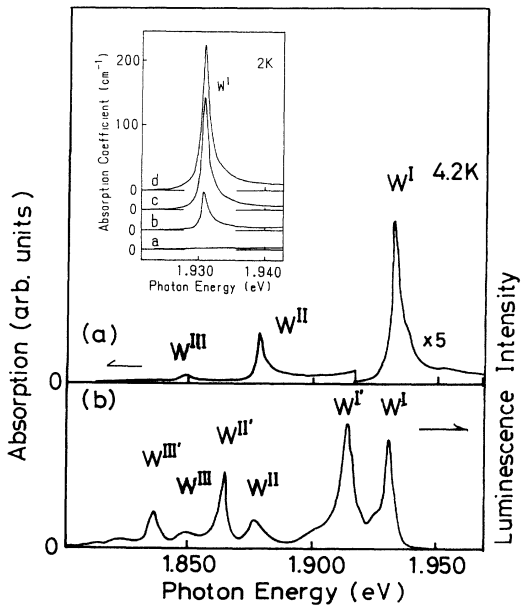

FIG. 1. (a) Absorption spectrum of the W^{I}, W^{II}, and W^{III} lines at 4.2 K. (b) Luminescence spectrum of the W^{I}, W^{II}, and W^{III} lines at 4.2 K. (Inset) Absorption spectra of a BiI_3 crystal under different conditions. Spectrum a was measured before deforming the crystal, and spectra b–d after deforming.

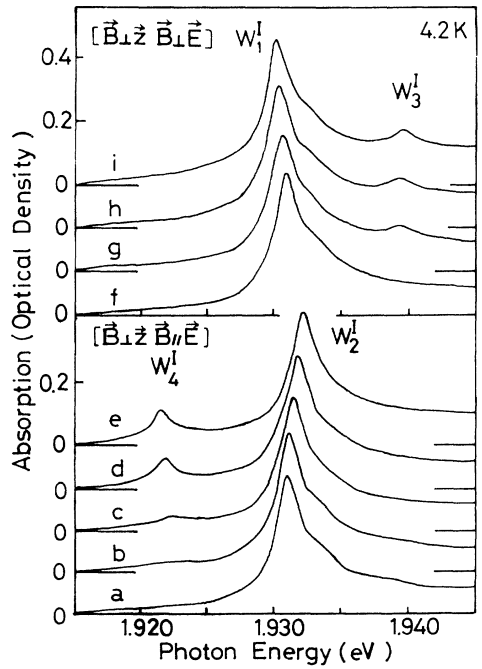

FIG. 2. The MA spectra of the W^{I} line at 4.2 K in both the [**B**⊥**z**, **B**||**E**, **k**||**z**] configuration (spectra b–e) and the [**B**⊥**z**, **B**⊥**E**, **k**||**z**] configuration (spectra g–i) with linearly polarized light: spectrum a, B=0 T; b, 11.6 T; c, 22.6 T; d, 33.6 T; e, 41.9 T; f, 0 T; g, 33.6 T; h, 37.8 T; i, 42.0 T.

the magnetic field. We labeled one located on the higher-energy side of W^{I} as W_3^{I}, and the other located on the lower-energy side of W^{I} as W_4^{I}. W_4^{I} was observed for $\mathbf{B}\|\mathbf{E}$, and W_3^{I} was observed for $\mathbf{B}\perp\mathbf{E}$. In the above, the split lines and the lines induced in the magnetic field have been distinguished by subscripts. As the magnetic field was increased, the absorption intensities of both the W_3^{I} and the W_4^{I} lines were increased, and the energy positions of the W_3^{I} and the W_4^{I} lines shift to the higher- and lower-energy sides, respectively. These four lines were simultaneously observed in the spectrum for the [$\mathbf{B}\perp\mathbf{z}$, $\mathbf{k}\|\mathbf{z}$] configuration obtained by using nonpolarized incident light.[8] The energy positions of the W_1^{I}, W_2^{I}, W_3^{I}, and W_4^{I} lines obtained by using linearly polarized light coincided with their respective values obtained by using nonpolarized light at the same magnetic field.

The energy positions of these four lines are plotted as a function of the square of the magnetic field in Fig. 3. It is found that the energy shifts of these lines in the $\mathbf{B}\perp\mathbf{z}$ configuration were proportional to B^2. The absorption intensities of the W_3^{I} and W_4^{I} lines in the $\mathbf{B}\perp\mathbf{z}$ configuration are plotted versus the square of the magnetic field in Fig. 4. These intensities were also proportional to B^2.

In the MA spectra in the [$\mathbf{B}\|\mathbf{z}$, $\mathbf{k}\|\mathbf{z}$] configuration, the energy position of the W_1^{I} line slightly shifts to the higher-energy side with increasing magnetic field. The value of the energy shift was about 0.2 meV at 40 T. No absorption line was observed at the energy positions of the W_3^{I} or the W_4^{I} lines even at the highest field of 41.8 T.

The splitting and growth of the new lines in the $\mathbf{B}\perp\mathbf{z}$ configuration were also observed in the MA spectra around the W^{II} line. The MA spectra in the [$\mathbf{B}\perp\mathbf{z}$, $\mathbf{B}\|\mathbf{E}$, $\mathbf{k}\|\mathbf{z}$] and the [$\mathbf{B}\perp\mathbf{z}$, $\mathbf{B}\perp\mathbf{E}$, $\mathbf{k}\|\mathbf{z}$] configurations are shown in Fig. 5. In the $\mathbf{B}\|\mathbf{E}$ configuration, the higher-energy component of the split lines and an induced line at the lower-energy side of W^{II} were observed, and these lines were labeled as W_2^{II} and W_4^{II}, respectively. In the

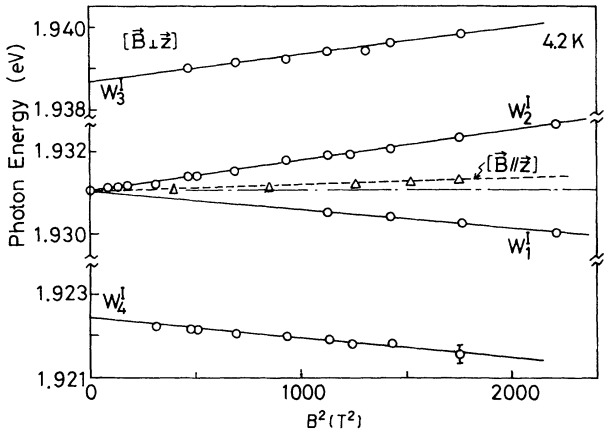

FIG. 3. Magnetic-field dependence of the energy position of the W_1^{I}, W_2^{I}, W_3^{I}, and W_4^{I} lines at 4.2 K. Open circles indicate the energy positions in the $\mathbf{B}\perp\mathbf{z}$ configurations, and open triangles indicate those in the $\mathbf{B}\|\mathbf{z}$ configuration. The dot-dashed line parallel to the abscissa is drawn to assist the view of the small energy shift.

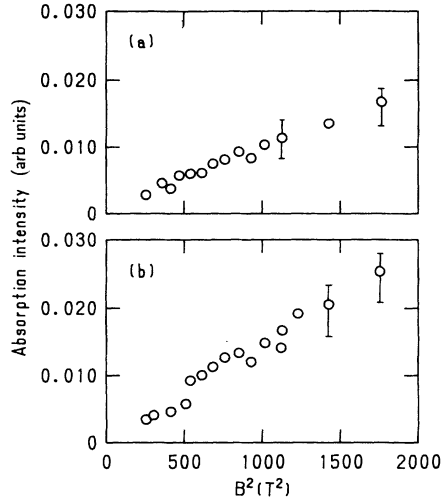

FIG. 4. Magnetic-field dependence of the absorption intensities of (a) the W_3^{I} and (b) the W_4^{I} lines in the $\mathbf{B}\perp\mathbf{z}$ configuration. The absorption intensities were obtained by subtracting the zero-field spectrum from each spectrum in a magnetic field and integrating the subtracted spectrum with respect to the photon energy.

$\mathbf{B}\perp\mathbf{E}$ configuration, the lower-energy component of the split lines and an induced line at the higher-energy side of W^{II} were observed, and these lines were labeled as W_1^{II} and W_3^{II}, respectively. The energy positions of W_2^{II} and W_3^{II} shift to higher energies with increasing magnetic field, and those of W_1^{II} and W_4^{II} shift to lower energies. The absorption intensities of both W_3^{II} and W_4^{II} increased

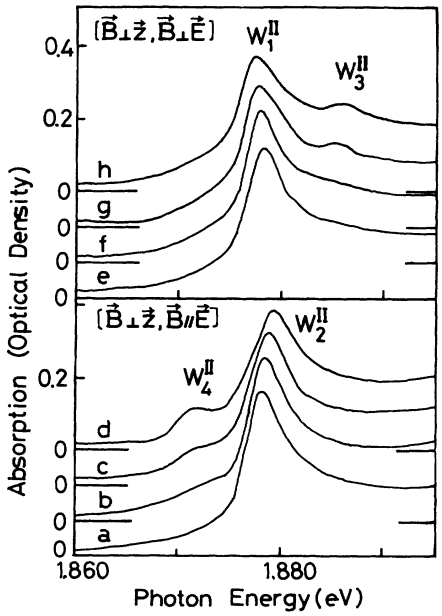

FIG. 5. The MA spectra of the W^{II} line at 4.2 K in both the [$\mathbf{B}\perp\mathbf{z}$, $\mathbf{B}\|\mathbf{E}$, $\mathbf{k}\|\mathbf{z}$] and the [$\mathbf{B}\perp\mathbf{z}$, $\mathbf{B}\perp\mathbf{E}$, $\mathbf{k}\|\mathbf{z}$] configurations with linearly polarized light: spectrum *a*, B=0 T; *b*, 20.8 T; *c*, 31.1 T; *d*, 40.0 T; *e*, 0 T; *f*, 20.5 T; *g*, 31.1 T; *h*, 40.0 T.

with increasing magnetic field in the same manner as W_3^{I} and W_4^{I}.

In the [$\mathbf{B}\|\mathbf{z}$, $\mathbf{k}\|\mathbf{z}$] configuration, the W^{II} line did not exhibit a drastic change. The W^{II} line did not show a splitting, and no absorption line was induced at the energy positions of the W_3^{II} or the W_4^{II} lines up to 40 T. As the magnetic field was increased, only a small shift to higher energy was observed.

C. Magnetoluminescence spectra

Magnetoluminescence spectra were also observed in a pulsed high magnetic field. Figure 6 shows the ML spectra around the W^{I} luminescence line in both the [$\mathbf{B}\perp\mathbf{z}$, $\mathbf{k}\|\mathbf{z}$] and the [$\mathbf{B}\|\mathbf{z}$, $\mathbf{k}\|\mathbf{z}$] configurations. The exciting light was the nonpolarized 514.5-nm line of an Ar-ion laser. The intensity of the luminescence line W^{I} was smaller than that of $W^{\mathrm{I}'}$ at zero magnetic field in the present sample. The spectra in the $\mathbf{B}\perp\mathbf{z}$ configuration showed a drastic change with increasing magnetic field. A luminescence line was induced by the magnetic field, and grew to become the strongest peak. The energy position of the line coincided with that of the W_4^{I} absorption line, which is denoted by a vertical bar in the figure. Thus the luminescence line can be assigned to W_4^{I}. The energy position of the W_4^{I} luminescence line shifts to the lower-energy side with increasing magnetic field, as does the W_4^{I} absorption line. In high magnetic fields, a small luminescence band appeared on the low-energy tail, and is labeled by $W_4^{\mathrm{I}'}$.

In the [$\mathbf{B}\|\mathbf{z}$, $\mathbf{k}\|\mathbf{z}$] configuration, no drastic change was observed even at 31.7 T as shown in Fig. 6. Thus the ML spectra showed the same anisotropy with respect to the magnetic field as did the MA spectra.

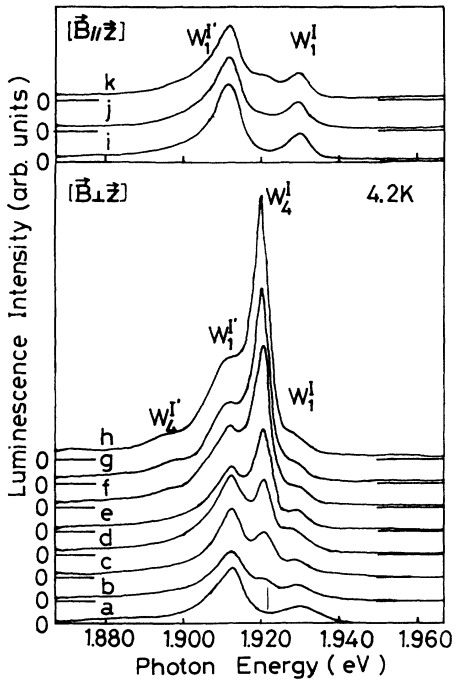

FIG. 6. The ML spectra of the W^{I} line with nonpolarized exciting light at 4.2 K in the [$\mathbf{B}\perp\mathbf{z}$, $\mathbf{k}\|\mathbf{z}$] configuration: spectrum *a*, B=0 T; *b*, 3.2 T; *c*, 6.5 T; *d*, 8.8 T; *e*, 17.4 T; *f*, 23.2 T; *g*, 28.9 T; *h*, 32.0 T, and in the [$\mathbf{B}\|\mathbf{z}$, $\mathbf{k}\|\mathbf{z}$] configuration: spectrum *i*, B=0 T; *j*, 17.6 T; *k*, 31.7 T. The vertical bar indicates the extrapolated energy of the W_4^{I} absorption line at B=0 T.

IV. DISCUSSION

A. The magnetic-field behavior

The W^{I}, W^{II}, and W^{III} transitions are induced by deforming the crystals. This fact suggests that the origin of the transitions is associated with a kind of disorder. Stacking disorders are frequently formed in layered crystals such as BiI_3. The optical spectra are generally influenced by the stacking disorders in the crystals.[12,13] For the W^J transitions, we propose a localized exciton model associated with a stacking disorder created by deforming the crystals. The present stacking disorder is different from the stacking fault described in Paper II.

First, we discuss the magnetic field effect on the W^J lines based on the cationic exciton model in the same way as for the bulk excitons in Paper I and for the stacking-fault excitons in Paper II.

We propose the following model for the origin of the W^{I} line. The W_1^{I}, W_2^{I}, W_3^{I}, and W_4^{I} lines are assigned to transitions to the states which originate from the cationic exciton states of BiI_3, ψ_6, ψ_{10}, ψ_3, and ψ_4, respectively. These four states are located in the band edge, and they are a $(x+iy)$-like, a $(x-iy)$-like, a z-like, and an almost pure triplet state, respectively.[3] W^{I} corresponds to a degenerate state composed of the W_1^{I} and the W_2^{I} states. In zero magnetic field, the transitions to W_3^{I} and W_4^{I} are optically forbidden in the present configuration.

In analogy to the bulk excitons, mixings between the W_2^{I} (originating from ψ_{10}) and the $W_4^{\mathrm{I}}(\psi_4)$ states and between the $W_1^{\mathrm{I}}(\psi_6)$ and the $W_3^{\mathrm{I}}(\psi_3)$ states take place by non-zero-spin Zeeman off-diagonal matrix elements in the $\mathbf{B}\perp\mathbf{z}$ configuration. Consequently, the degeneracy of the W_1^{I} and the W_2^{I} states is lifted, and the transitions to the W_3^{I} state and the W_4^{I} state become partially allowed by the mixings. Taking the linear Zeeman Hamiltonian term as a perturbation and calculating the first- and the second-order terms, in the $\mathbf{B}\perp\mathbf{z}$ configuration, we find that the energy shifts of the four lines are proportional to B^2, and that the absorption intensities of the W_3^{I} and the W_4^{I} lines are also proportional to B^2. These results are consistent with the experimental data shown in Figs. 3 and 4. The effective g value in the $\mathbf{B}\perp\mathbf{z}$ configuration ($g_{\mathrm{eff}}^{\perp}$) is estimated to be 1.2. The present value obtained for the W^{I} exciton is different from that of the bulk excitons ($g_{\mathrm{eff}}^{\perp}$=1.6).[3]

According to the cationic exciton model, the selection rule in the $\mathbf{B}\perp\mathbf{z}$ configuration is such that the transitions to ψ_4 and ψ_{10} are allowed for $\mathbf{B}\|\mathbf{E}$, and those to ψ_3 and ψ_6 are allowed for $\mathbf{B}\perp\mathbf{E}$.[3] In the experiments, W_4^{I} (originating from ψ_4) and W_2^{I} (ψ_{10}) were allowed for $\mathbf{B}\|\mathbf{E}$, while W_3^{I} (ψ_3) and W_1^{I} (ψ_6) were allowed for $\mathbf{B}\perp\mathbf{E}$. These observations are consistent with the selection rule.

In the $\mathbf{B}\|\mathbf{z}$ configuration, there is no off-diagonal matrix element among the states ψ_i.[3] Therefore, it is reasonable that we have observed a very small energy shift of the W^{I} line and neither the W_3^{I} nor the W_4^{I} lines in the MA spectra of the $\mathbf{B}\|\mathbf{z}$ configuration.

The luminescence line W^{I} was observed in zero field. The luminescence line W_4^{I} was observed in the $\mathbf{B}\perp\mathbf{z}$ configuration. The luminescence intensity of W_4^{I} was much larger than those of the W_1^{I} and the W_2^{I} lines in high magnetic fields. This feature is different from the MA spectra. This difference can be understood in the following way. In general, the intensity of exciton luminescence is proportional both to the occupation number of the exciton state and to the radiative transition probability between the exciton and the ground states. Since the W_4^{I} state is almost a triplet state, the radiative decay time of the W_4^{I} state is expected to be much larger than those of the W_1^{I} and W_2^{I} states. If the relaxation process of the W_1^{I} or the W_2^{I} exciton state is dominated by a relaxation process to the W_4^{I} state, the occupation number of the W_4^{I} state becomes much larger than those of the W_1^{I} and W_2^{I} states. The larger occupation number and the nonzero transition probability of W_4^{I} in magnetic fields could result in an enhanced luminescence intensity of W_4^{I} in spite of the smaller transition probability than those of W_1^{I} and W_2^{I}. In the MA spectra, the W^{I} line splits into two lines for $\mathbf{B}\perp\mathbf{z}$, whereas splitting of the luminescence line was not discernible in the present spectra for $\mathbf{B}\perp\mathbf{z}$. This is due to the broader linewidth of the luminescence lines compared to the absorption lines, or due to the small luminescence intensity of W_2^{I} because of a relaxation process of the W_2^{I} state to lower-lying states.

The behavior of the W^{II} line in magnetic fields has the same character as that of the W^{I} line. In analogy to the case of W^{I}, the W_1^{II}, W_2^{II}, W_3^{II}, and W_4^{II} states are assigned to originate from the cationic exciton states ψ_6, ψ_{10}, ψ_3, and ψ_4, respectively. The origin of the W^{II} line is the transition to a degenerate state composed of two states W_2^{II} and W_1^{II} in zero field. Mixings between W_1^{II} and W_3^{II} and between W_2^{II} and W_4^{II} take place in the $\mathbf{B}\perp\mathbf{z}$ configuration. By the mixing, the degeneracy is lifted, and the transitions to the W_3^{II} state and the W_4^{II} state become partially allowed. The observed selection rule of the transitions to the W_i^{II} states for $\mathbf{B}\perp\mathbf{z}$ is also consistent with the cationic exciton model. $g_{\mathrm{eff}}^{\perp}$ is estimated to be 1.1 for W^{II}. This value is roughly equal to that for W^{I}.

From the considerations shown above for the MA and the ML spectra, both W^{I} and W^{II} can be attributed to exciton transitions which originate from the cationic exciton states.

According to the effective-mass approximation for Wannier excitons, we should observe a diamagnetic shift proportional to the square of the exciton radius in magnetic fields. The radius of the band-edge exciton in BiI_3 is estimated to be as small as the thickness of the unit layer.[6] The very small magnetic shift of the W^{I} and W^{II} lines in the $\mathbf{B}\|\mathbf{z}$ configuration suggests that the radii of the excitons are also very small compared with the usual excitons in semiconductors. Assuming that the magnetic shift of the W^{I} line ($\sim$0.2 meV at 40 T) for $\mathbf{B}\|\mathbf{z}$ is entirely due to the diamagnetic shift, the radius of the $1s$ exciton was estimated to $\sim$10 Å, where we use the dielectric constant ($\sim$6.1) estimated by Kaifu[6] for the bulk crystals. As definite anisotropic parameters for the band-edge exciton have not been obtained, we assume an isotropic exciton state.

B. Model of the W^J transitions

In the previous section, it has been shown that the origins of the W^{I} and W^{II} lines are cationic exciton states. In this section, we propose a complete model for the W^J (J=I,II,III) transitions to explain their differences.

The regular layer arrangement of BiI_3 single crystals is represented as $ABCABCABC\ldots$ (called the $3R$ structure[7,14]) where $A \equiv \alpha\beta^A\gamma$, $B \equiv \alpha\beta^B\gamma$, and $C \equiv \alpha\beta^C\gamma$ are different arrangements of the unit layers, as described in Paper I. In the case that one A layer stacks directly above another A layer, the $3R$ structure has a break between the two A layers. This kind of stacking creates a stacking disorder in BiI_3. The stacking disorder gives an arrangement $ABC\underline{AA}BCABC\ldots$ (labeled as arrangement SD-1), that is, the stacking disorder exists at the interface between the two unit layers underlined. If stacking disorders occur successively, the arrangement becomes $ABC\underline{AAA}BCABC\ldots$ (arrangement SD-2). Similarly, three successive stacking disorders gives an arrangement $ABC\underline{AAAA}BCABC\ldots$ (arrangement SD-3).

In the present model, the origins of the W^{I}, W^{II}, and W^{III} transitions are assigned to be excitons localized around the layer arrangements SD-1, SD-2, and SD-3, respectively. The deformation by the bending stress makes stacking disorders, and brings about perturbed states originating from the bulk exciton states. At the stacking disorders, the translational symmetry is broken along the z direction, while a new translational symmetry different from that of the regular stacking region should be formed in the plane perpendicular to the z direction. Accordingly, the excitons cannot regularly propagate along the z direction at the stacking disorder, while they can propagate in the plane perpendicular to the z direction. Thus, the exciton states are regarded as confined in the plane around the stacking disorder.

The nature of the W^J lines is different from those of the Q, R, S, and T lines, which are also associated with stacking faults. The MA spectra of the Q, R, S, and T lines depend on the angle θ between the direction of the magnetic field and the x axis of the crystal in the $\mathbf{B}\perp\mathbf{z}$ configuration, as described in Paper II, while such a θ dependence was not observed in the MA spectra of the W^J transitions and the bulk exciton transitions. This difference can be ascribed to the symmetry of the stacking disorder related to the W^J line, which should be simpler than that of the stacking fault for the Q, R, S, and T lines.[4]

Based on the above considerations, a calculation of the energy level of the W^J lines was attempted. In the following, we adopt a one-dimensional tight-binding model to consider only the z direction. The Hamiltonian of this model is given by

$$H = \sum_n \varepsilon(n) a_n^\dagger a_n + \sum_n \sum_{>m} T(n,m)(a_n^\dagger a_m + a_m^\dagger a_n),$$

$$n, m = 1, 2, 3, ..., N,$$

where $a_n^\dagger$ and a_n are the creation and annihilation operators for the exciton in the nth unit layer, respectively. N is the number of unit layers of a crystal. The first and the second terms are the site and the transfer energies of the exciton, respectively. In a perfect crystal, both $\varepsilon(n)$ and $T(n,m)$ should be independent of site. In the present model for the stacking disorder, $\varepsilon(n)$ and $T(n,m)$ are taken as follows:

$$\varepsilon(n) = \varepsilon_0,$$

$$T(n,m) = \begin{cases} 0 & (n \neq m+1), \\ T_W & (n = m+1, n = N_0+1, N_0+2, ..., N_0+N_D), \\ T_{\text{bulk}} & (n = m+1, n \neq N_0+1, N_0+2, ..., N_0+N_D), \end{cases}$$

$$T(N,1) = T_{\text{bulk}}.$$

The last relation represents a cyclic boundary condition. The stacking disorders successively exist between the N_0th and the (N_0+N_D)th layers; N_D=1 for SD-1, N_D=2 for SD-2, and N_D=3 for SD-3. The central energy of the exciton band is given by ε_0, and the exciton bandwidth along the K_Z direction (K_Z is a wave vector parallel to the z direction) is four times as large as T_{bulk}. The energy level of the W^J lines is given as the lowest eigenvalues. In the present numerical computation, N was taken to be 50, and it is sufficiently large for calculating the lowest eigenvalue. The calculated values are plotted in Fig. 7, and are roughly in agreement with the experimental values. The calculated values were obtained by using the following values: ε_0=2.040 eV, T_W=0.116 eV, and T_{bulk}=0.016 eV. The values of ε_0 and T_{bulk} were uniquely determined by the exciton band of the K_Z direction.[3] Therefore, only T_W is a fitting parameter in the present calculation. T_W became about seven times as large as T_{bulk}. According to the present stacking-disorder model, the interlayer distance of two bismuth ions (cations), whose electrons govern the character of the band-edge exciton states, becomes shorter at the stacking disorder compared with the regular stacking region. The radii of the present excitons are comparable with the interlayer distance. Thus a change of this distance results in the striking change of the transfer energy at the stacking disorder.

The existence probability of excitons for each lowest eigenstate is shown for SD-1, SD-2, and SD-3 in Fig. 8. In the case of arrangement SD-1, the exciton is almost confined in two unit layers at the stacking disorder. The exciton is almost confined in three unit layers and in four unit layers in the cases of SD-2 and SD-3, respectively. The change of the transfer energy causes the localization of excitons in the present model.

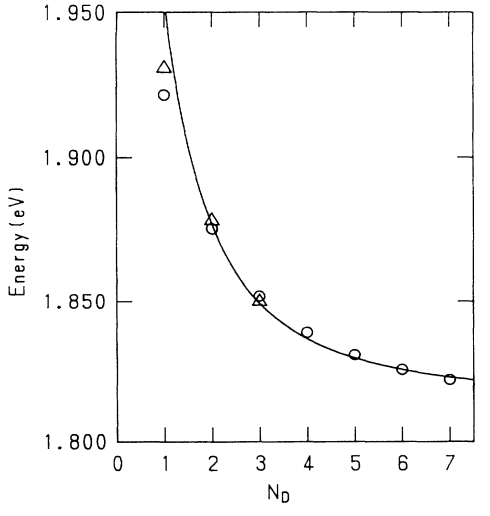

FIG. 7. Energy level of the W^J lines. Triangles and circles represent experimental data and values calculated by the tight-binding model, respectively. Solid line represents the fitting curve by the equation in the text.

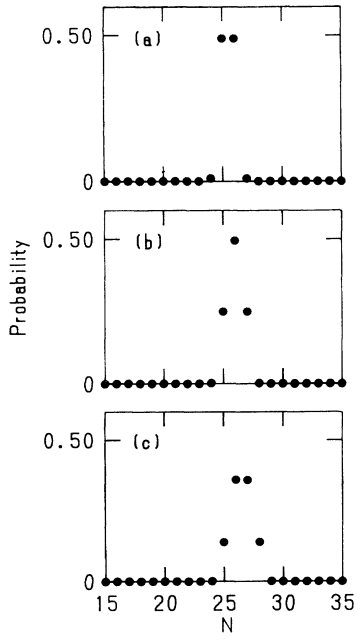

FIG. 8. Calculated existence probability of each lowest eigenstate for (a) N_D=1, (b) N_D=2, and (c) N_D=3. N_0 is taken as 25.

As J is decreased, the wave function of the exciton is confined in a narrower region in the z direction, and the energy of the excitons shifts to the higher-energy side. We fit the energy positions of the W^J with the following equation which describes a quantum size effect,

$$E = \frac{\pi^2\hbar^2}{2M_Z L_Z^2} + E_W.$$

The thickness of one A layer in the z direction is 6.9 Å. Since the W^{I} exciton is almost confined in two unit layers according to the above calculation of the existence probability, L_Z is taken as 13.8 Å for SD-1. In the same way, L_Z is taken as 20.7 Å for SD-2 and 27.7 Å for SD-3. If a BiI_3 crystal having such a layer arrangement $AAAAAA\ldots$ were present, the space symmetry of the crystal should be D_{3d}^1, while the space symmetry of the crystal in the present work is C_{3i}^2. We may regard an ultrathin crystal having space symmetry D_{3d}^1 to exist in a bulk crystal having C_{3i}^2 symmetry. E_W is the energy of the exciton band bottom in a hypothetical D_{3d}^1 crystal.

The fitting curve is shown in Fig. 7, and it agrees roughly with the values calculated by the present tight-binding model except for SD-1. The mass of the exciton in the K_Z direction M_Z is a fitting parameter, and was obtained as $1.4m_e$. It is not a reduced mass but a translational mass in the present model.

V. CONCLUSION

A series of absorption lines W^J (J=I,II,III) were observed in BiI_3 single crystals deformed by a bending stress. The W^J lines have sharp line widths. Owing to the sharpness, very small energy shift and splitting were detected in the magnetic fields. From the analysis of the MA and ML spectra of the lines, the origin of the lines is ascribed to exciton states localized around a stacking disorder. The exciton states have the character of cationic exciton states. It was proposed that the W^{I}, W^{II}, and W^{III} lines arise from exciton states confined in three specific kinds of regions having different thicknesses. The excitons exhibit a quantum size effect, and the energy level of the excitons can be described by two simple models.

ACKNOWLEDGMENTS

This work is partially supported by a Grant-in Aid for Scientific Research from the Ministry of Education, Science and Culture in Japan. The authors would like to thank Professors Y. Kaifu and T. Karasawa for their encouragement throughout this work.

*Permanent address: Department of Physics, Faculty of Liberal Arts and Education, Yamanashi University, Takeda, Kofu 400, Japan.

†Present address: Department of Materials, Faculty of Science, Himeji Institute of Technology, Harima-Kagakukoen, Hyogo 678-12, Japan.

‡Present address: Department of Natural Science, Osaka Women's University, Daisen, Sakai 590, Japan.

[1]Y. Kaifu and T. Komatsu, J. Phys. Soc. Jpn. **40**, 1377 (1976).

[2]T. Komatsu and Y. Kaifu, J. Phys. Soc. Jpn. **40**, 1062 (1976).

[3]S. Takeyama, K. Watanabe, N. Miura, T. Komatsu, K. Koike, and Y. Kaifu, Phys. Rev. B **41**, 4512 (1990).

[4]T. Komatsu, K. Koike, Y. Kaifu, S. Takeyama, K. Watanabe, and N. Miura, Phys. Rev. B **48**, 5095 (1993).

[5]T. Komatsu, Y. Kaifu, S. Takeyama, and N. Miura, Phys. Rev. Lett. **58**, 2259 (1987).

[6]Y. Kaifu, J. Lumin. **42**, 61 (1988).

[7]Y. Kaifu, T. Komatsu, and T. Aikami, Nuovo Cimento B **38**, 449 (1977).

[8]K. Watanabe, S. Takeyama, T. Komatsu, N. Miura, and Y. Kaifu, in *High Magnetic Fields in Semiconductor Physics II*, edited by G. Landwahr (Springer-Verlag, Tokyo, 1989), p. 301.

[9]M.P. Lisitsa and F.V. Motsnyi, Ukr. Fiz. Zh. **21**, 1025 (1976).

[10]See, for example, Y. Kayanuma, Phys. Rev. B **44**, 13 085 (1991); E. Hanamura, *ibid.* **37**, 1273 (1988).

[11]Y. Nagamune, S. Takeyama, and N. Miura, Phys. Rev. B **43**, 12 401 (1991).

[12]J.J. Fourney, K. Mascheke, and E. Mooser, J. Phys. C **10**, 1887 (1975).

[13]Y. Sasaki and Y. Nishina, Physica B **105**, 45 (1981).

[14]R.W.G. Wyckoff, *Crystal Structure*, 2nd ed. (Interscience, New York, 1964), Vol. 2, p. 45.